Adsorption and Co-adsorption of Ethylene and Carbon Monoxide on Silica-Supported Monodisperse Pt Nanoparticles: Volumetric Adsorption and Infrared Spectroscopy Studies

Robert M. Rioux,[†] James D. Hoefelmeyer,[‡] Michael Grass, Hyunjoon Song,[§] Krisztian Niesz,[||] Peidong Yang, and Gabor A. Somorjai*

Department of Chemistry, University of California, Berkeley and Lawrence Berkeley National Laboratory, Materials and Chemical Sciences Divisions, Berkeley, California 94720

Received August 30, 2007. In Final Form: September 30, 2007

The adsorption of carbon monoxide and ethylene, and their sequential adsorption, was studied over a series of Pt/SBA-15 catalysts with monodisperse particle sizes ranging from 1.7 to 7.1 nm by diffuse-reflectance infrared spectroscopy and chemisorption. Gas adsorption was dependent on the Pt particle size, temperature, and sequence of gas exposure. Adsorption of CO at room temperature on Pt/SBA-15 gives rise to a spectroscopic feature assigned to the C−O stretch: ν(CO) = 2075 cm^{-1} (1.9 nm); 2079 cm^{-1} (2.9 nm); 2082 cm^{-1} (3.6 nm); and 2090 cm^{-1} (7.1 nm). The intensity of the signal decreased in a sigmoidal fashion with increasing temperature, thereby providing semiquantitative surface coverage information. Adsorption of ethylene on Pt/SBA-15 gave rise to spectroscopic features at ∼1340, ∼1420, and ∼1500 cm^{-1} assigned to ethylidyne, di-σ-bonded ethylene, and π-bonded ethylene, respectively. The ratio of these surface species is highly dependent on the Pt particle size. At room temperature, Pt particles stabilize ethylidyne as well as di-σ- and π-bonded ethylene; however, ethylidyne predominated on the surfaces of larger particles. Ethylidyne was the only identifiable species at 403 K, with its formation being more facile on larger particles. Co-adsorption experiments reveal that the composition of the surface layer is dependent on the order of exposure to gases. Exposure of a C_2H_4-covered Pt surface to CO resulted in an ∼50% decrease in chemisorbed CO compared to a fresh Pt surface. The ν(CO) appeared at 2050 cm^{-1} on Pt/SBA-15 pretreated with C_2H_4 at room temperature. The di-σ-bonded and π-bonded species are the most susceptible to displacement from the surface by CO. The formation of ethylidyne appeared to be less sensitive to the presence of adsorbed carbon monoxide, especially on larger particles. Upon exposure of C_2H_4 to a CO-covered Pt surface, little irreversible uptake occurred due to nearly 100% site blocking. These results demonstrate that carbon monoxide competes directly with ethylene for surface sites, which will have direct implications on the poisoning of the heterogeneously catalyzed conversion of hydrocarbons.

1. Introduction

Lateral interactions between surface species formed upon adsorption lead to kinetic phenomena, which may deviate from conventional theory, such as Langmuir−Hinshelwood heterogeneous kinetics.[1,2] Interactions between adsorbates can lead to well-ordered surface structures, to disordered structures, and to surface adsorbate islanding.[2] These phenomena can span length scales ranging from a few atomic diameters to mesoscale dimensions.[3] Many of these phenomena originate or terminate at defect sites; therefore, the role of surface roughness (nanoparticle size) on adsorbate−adsorbate interactions is important. Conventional theories, such as the Langmuir isotherm, have been modified to account for the nonuniformity of a real surface and intermolecular interactions between adsorbates. The Temkin isotherm[4] deviates from the previous theory in that it accounts for reduced adsorption (linearly) as a function of coverage. Nonuniform dynamic (spatially, energetically, and temporally) interactions between adsorbates on surfaces have a tremendous impact on observed heterogeneous reaction kinetics by influencing the stability of transition states, modifying adsorption geometries, and perturbing the adsorbate−surface bonding.[5] The influence of intermolecular interactions, within a homogeneous surface adlayer, on adsorption dynamics and kinetics has been studied extensively; however, intermolecular interactions have been studied to a lesser extent within a heterogeneous surface adlayer (different reactants) even though they play a critical role in heterogeneous catalysis at high pressures. Due to the large number of studies of the surface chemistry of CO and ethylene on Pt single crystals, co-adsorption of CO/C_2H_4 on supported Pt particles is well-suited for investigation.[6] In this paper, the influence of Pt particle dimension, within a series of Pt/SBA-15 materials, on the adsorption of carbon monoxide and ethylene was investigated. The implication of particle size on the co-adsorption of ethylene and carbon monoxide is extended to the hydrogenation of ethylene in low pressures of carbon monoxide in a separate manuscript.[7] This study demonstrates that Pt particle size does not influence the resistance of a hydrocarbon conversion catalyst to poisoning by a strong adsorbate and should not be used as a parameter for the design of a CO-tolerant catalyst.

* To whom correspondence should be addressed. E-mail: somorjai@berkeley.edu.

[†] Current address: Department of Chemistry and Chemical Biology, Harvard University, Cambridge, Massachusetts 02138.

[‡] Current address: Department of Chemistry, University of South Dakota, Vermillion, South Dakota 57069.

[§] Current address: Department of Chemistry and School of Molecular Science (BK21), Korea Advanced Institute of Science and Technology, Daejeon 305-701, Korea.

[||] Current Address: ThalesNano Inc., Zahony u. 7., H-1031 Budapest, Hungary.

(1) Zaera, F. *Acc. Chem. Res.* **2002**, *35*, 129.
(2) Wintterlin, J. *Adv. Catal.* **2000**, *45*, 131.
(3) Sachs, C.; Hildebrand, M.; Volkening, S.; Wintterlin, J.; Ertl, G. *Science* **2001**, *293*, 1635.
(4) McCash, E. M. *Surface Chemistry*; Oxford University Press: New York, 2001.
(5) Rudziński, W.; Steele, W. A. *Equilibria and Dynamics of Gas Adsorption on Heterogeneous Solid Surfaces*; Elsevier: Amsterdam, 1997; Vol. 104, p 1.
(6) Somorjai, G. A. *Introduction to Surface Chemistry and Catalysis*; J. Wiley & Sons: New York, 1994.

10.1021/la702685a CCC: $40.75
Published on Web 12/06/2007

2. Experimental Section

2.1. Catalyst Synthesis and Characterization. A series of ~3% Pt(*X*)/SBA-15 (*X* = 1.7, 2.9, 3.6, and 7.1 nm) catalysts were used in these experiments. A detailed description of their synthesis and characterization can be found elsewhere.[8,9] Briefly, nearly monodisperse Pt nanoparticles between 1.7 and 7.1 nm were synthesized in the presence of a surface templating polymer, poly(vinylpyrrolidone) (PVP), by a modified alcohol reduction method. Number-average particle sizes with standard deviations after counting ≥200 particles were 1.73 ± 0.26 (1.7), 2.80 ± 0.21 (2.9), 3.39 ± 0.26 (3.6), and 7.16 ± 0.37 (7.1) nm by TEM (line-broadening XRD analysis), indicating high uniformity and monodispersity of each particle less than $\sigma \sim 8\%$.[8] After synthesis and purification of the nanoparticles, they were encapsulated in mesoporous silica (SBA-15) by direct participation in the hydrothermal reaction. Synthesis of SBA-15[10] was conducted at neutral pH using NaF as a catalyst for hydrolysis of the silica precursor, tetramethyl orthosilicate (TMOS).[11] The mechanism of nanoparticle encapsulation has been previously discussed.[9] *Ex situ* calcination in O_2 at 623 or 723 K for 24−36 h (sample dependent) was used to remove PVP from the particle surface; 1.7 nm particles are calcined at 623 K for 24 h to prevent particle sintering, while 36 h at 723 K is required for the catalyst containing 7.1 nm particles. Typically, 300−400 mg of Pt(*X*)/SBA-15 was calcined in a horizontal tube furnace at the specified temperature and time in 100 cm^3 (normal temperature and pressure (NTP)) min^{-1} of 20% O_2/He (UHP both gases, Praxair). Calcined samples were stored in scintillation vials prior to use. Metal loadings were determined by inductively coupled plasma-optical emission spectroscopy (ICP-OES) (Galbraith Laboratories, Knoxville, TN).

A 3.2% Pt/SiO_2 catalyst prepared by ion exchange of $Pt(NH_3)_4(OH)_2 \cdot xH_2O$[12] and an ultrahigh purity (UHP) Pt powder (Alfa Aesar, 1 μm particle size) were used as standard samples for both chemisorption and infrared spectroscopy measurements. The ultrahigh purity Pt powder was cleaned by heating at 473 K for 0.5 h in 20% O_2/He to remove any surface contaminants before reduction. A 2% Pt/Al_2O_3 (Exxon Research and Engineering) sample was included to determine if the support influenced co-adsorption behavior. A thoroughly characterized 6.3% Pt/SiO_2 (EUROPT-1) catalyst with the Pt particle size distribution centered at 1.8 nm was also included.[13−18]

2.2. Volumetric Gas Adsorption Measurements. Selective chemisorption measurements were conducted to determine the dispersion of each sample. An automated volumetric physisorption/chemisorption analyzer (Quantachrome Autosorb-1) with *in situ* pretreatment capabilities was used. All catalysts were activated in 50 cm^3 (NTP) He min^{-1} at 473 K for 1 h, followed by reduction in 50 cm^3 (NTP) H_2 min^{-1} at 673 K for 75 min. Prior to chemisorption measurements, catalyst samples were evacuated for 1 h at 623 K and cooled to room temperature under vacuum. H_2, CO, and H_2-O_2 isotherms were collected on the same sample (~300 mg). After the initial reduction, catalysts were heated (10 K min^{-1}) in He to 673 K and reduced with 50 cm^3 (NTP) H_2 min^{-1} for 0.5 h. Adsorption uptakes extrapolated to zero pressure (monolayer uptake) were used to calculate metal dispersion (*D*). Spherical particle sizes were calculated from dispersion measurements, $d\,(\text{nm}) = 1.13/D$, assuming a Pt atom surface density of 1.27×10^{19} m^{-2}.[19]

Co-adsorption experiments of CO and C_2H_4 were conducted at 298 and 403 K on catalyst samples pretreated as previously described. Adsorption experiments were sequential: CO adsorption followed by C_2H_4 adsorption and vice versa. After pretreatment, total and reversible isotherms of one adsorbate with an interim 1 h evacuation between isotherms were collected at either 298 or 403 K. After a 1 h evacuation following the reversible isotherm of the first adsorbate, dual isotherms were measured for the second adsorbate. Experiments at 298 and 403 K were conducted on the same sample (~300 mg): the 298 K experiment followed by the 403 K experiment. Samples were subjected to a 0.5 h oxidation in 50 cm^3 (NTP) O_2 min^{-1}, followed by a 0.5 h reduction in 50 cm^3 (NTP) H_2 min^{-1} at 573 K before beginning the 403 K isotherm set.

2.3. Infrared Measurements of CO and C_2H_4 Adsorption. The adsorption of CO and C_2H_4 on various silica-supported Pt catalysts was studied with *in situ* diffuse-reflectance infrared Fourier transform spectroscopy (DRIFTS), using a Nicolet Nexus 670 spectrometer equipped with a Thermo Spectra-Tech controlled atmosphere diffuse reflection cell. A Pt/SiO_2 catalyst (~50 mg for amorphous SiO_2, ~10 mg SBA-15 samples) was loaded in the diffuse-reflectance cell and given a pretreatment identical to those used for chemisorption and catalytic studies[7] with a gas manifold equipped with mass flow controllers (Porter Instruments Company) connected to the diffuse-reflectance cell. He (99.999%, Praxair), 10% H_2/He (99.999% both gases, Praxair), CO (99.9%, Airgas), and C_2H_4 (99.9%, Praxair) were used without further purification. A single beam spectrum (128 scans, 2 cm^{-1} resolution) of the freshly reduced catalyst was obtained at 300 K under 30 cm^3 (NTP) He min^{-1} and used as the background for subtraction of silica features for all samples in the presence and absence of gas-phase CO and/or ethylene at 300 K. The sample was then exposed to a 30 cm^3 (NTP) min^{-1} mixture of 10% CO/He or 10% C_2H_4/He for 30 min at 300 K, followed by purging in 30 cm^3 (NTP) He min^{-1} at 300 K. Gas-phase spectra of CO and ethylene were taken in the DRIFTS cell using a Au mirror.

3. Results

3.1. Catalyst Characterization. Metal particle sizes were determined by transmission electron microscopy (TEM), X-ray diffraction (XRD), and selective gas adsorption. Table 1 is a compilation of the adsorption uptakes of H_2, CO, and O_2 as well as the titration of O_{ad} by H_2 ($Pt_s\text{-}O + 3/2H_2 \rightarrow Pt_s\text{-}H + H_2O$).[20] Line-broadening XRD techniques used to calculate Pt particle sizes from the full width at half-maximum (fwhm) of the Pt(111) Bragg reflection are in good agreement with chemisorption measurements. The particle size determined by chemisorption is always larger than TEM or XRD particle sizes; we believe this is due to residual PVP on the surface of the particles.

Assuming the number of surface atoms, Pt_s counted by H_2-O_2 titration is the most accurate measurement of dispersion, the ratio CO_{Irr}/Pt_s was calculated. Previous experiments[21] have established $CO_{irr}/Pt_s = 0.68$ on Pt(111). The adsorption of CO to step edges and kink sites of high-index single crystals leads to a CO/Pt ratio of unity. Nanocrystals larger than 4 nm tend to exhibit faceting with surfaces terminated by low-index surface planes, whereas, below 4 nm, surfaces become roughened. The larger nanocrystals should yield CO_{irr}/Pt_s values near 0.68, with this value increasing as particle size decreases (or as lattice regularity decreases). The Pt/SiO_2 and Pt/SBA-15 materials yield CO_{irr}/Pt_s values of 0.61−0.94, with a trend of decreasing CO_{irr}/Pt_s with increasing particle size. The data are consistent with the

(7) Rioux, R. M.; Komor, R.; Song, H.; Hoefelmeyer, J. D.; Grass, M.; Niesz, K.; Yang, P.; Somorjai, G. A. *J. Catal.* [Online early access]. DOI: 10.1016/j.j.cat.2007.10.1015.
(8) Rioux, R. M.; Song, H.; Hoefelmeyer, J. D.; Yang, P.; Somorjai, G. A. *J. Phys. Chem. B* **2005**, *109*, 2192.
(9) Song, H.; Rioux, R. M.; Hoefelmeyer, J. D.; Komor, R.; Niesz, K.; Grass, M.; Yang, P. D.; Somorjai, G. A. *J. Am. Chem. Soc.* **2006**, *128*, 3027.
(10) Zhao, D. Y.; Feng, J. L.; Huo, Q. S.; Melosh, N.; Frederickson, G. H.; Chmelka, B. F.; Stucky, G. D. *Science* **1998**, *279*, 548.
(11) Kim, J. M.; Han, Y.-J.; Chmelka, B. F.; Stucky, G. D. *Chem. Commun.* **2000**, *24*, 2437.
(12) Singh, U. K.; Vannice, M. A. *J. Catal.* **2000**, *191*, 165.
(13) Bond, G. C.; Wells, P. B. *Appl. Catal.* **1985**, *18*, 221.
(14) Bond, G. C.; Wells, P. B. *Appl. Catal.* **1985**, *18*, 225.
(15) Frennet, A.; Wells, P. B. *Appl. Catal.* **1985**, *18*, 243.
(16) Geus, J. W.; Wells, P. B. *Appl. Catal.* **1985**, *18*, 231.
(17) Wells, P. B. *Appl. Catal.* **1985**, *18*, 259.
(18) Gnutzmann, V.; Vogel, W. *J. Phys. Chem.* **1990**, *94*, 4991.
(19) Anderson, J. R. *Structure of Metallic Catalysts*; Academic Press: New York, 1975.
(20) Benson, J. E.; Boudart, M. *J. Catal.* **1965**, *4*, 704.
(21) Vestergaard, E. K.; Thostrup, P.; An, T.; Lægsgaard, E.; Stensgaard, I.; Hammer, B.; Besenbacher, F. *Phys. Rev. Lett.* **2002**, *88*, 259601.
(22) Hardeveld, R. V.; Hartog, F. *Surf. Sci.* **1969**, *15*, 189.

Table 1. Adsorption Uptake and Particle Size Determined by Chemisorption, TEM, and XRD Techniques

	probe gas uptakes[c] (μmol g^{-1})						particle size, *d* (nm)		
	H_2	CO		O_2	H_2-O_2	dispersion, *D*	chemisorption[d]		
catalyst[a,b]	total	total	irrev	irrev	total	H_2-$O_{2,total}$	H_2	H_2-O_2	XRD[e]
3.2% Pt/SiO_2-IE	133.1	166.7	152.2	24.2	262.0	1	1	1	
6.3% Pt/SiO_2 (EUROPT-1)	151.2	182.0	175.0	94.6	334.0	0.69	1.2	1.6	1.8[f]
2% Pt/Al_2O_3-Exxon	43.5	80.6	70.1	17.4	66.1	0.43	1.3	2.6	3.4
2.33% Pt(1.7 nm)/SBA-15	29.8	66.1	59.6	21.9	94.9	0.53	2.3	2.1	1.7
2.69% Pt(2.9 nm)/SBA-15	21.0	39.5	34.9	15.4	76.2	0.37	3.7	3.1	2.9
2.62% Pt(3.6 nm)/SBA-15	16.6	32.8	30.7	12.9	51.9	0.26	4.6	4.4	3.7
2.86% Pt(7.1 nm)/SBA-15	9.4	14.7	11.7	12.2	28.4	0.13	8.8	8.7	7.3
UHP Pt powder	16.7	15.1	13.7	8.6	30.3	0.004	173.5	286.5	>100

[a] Actual metal loading determined by ICP-OES. [b] Number average particle size for SBA-15 materials. Determined by counting a minimum of 200 free-standing particles. [c] Conducted at 298 K. [d] Determined by $1.13/(Pt_s/Pt_T)$. [e] Based on the Scherrer−Debye equation after subtracting the SBA-15 baseline. [f] Taken from ref 18.

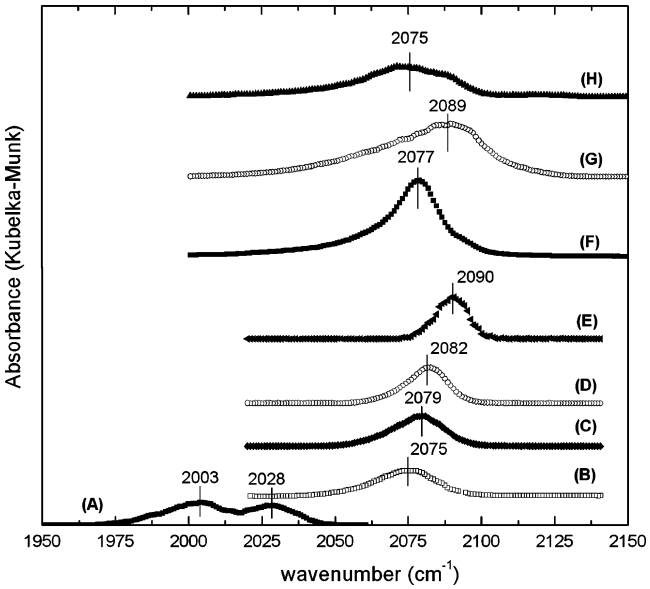

Figure 1. Diffuse-reflectance infrared spectra of CO adsorbed at 298 K on Pt(*X*)/SBA-15: (A) SBA-15 support, (B) $X = 1.7$ nm particles, (C) $X = 2.9$ nm particles, (D) $X = 3.6$ nm particles, (E) $X = 7.1$ nm particles, (F) 3.2% Pt/SiO_2, (G) 6.3% Pt/SiO_2 (EUROPT-1), and (H) 2% Pt/Al_2O_3.

higher proportion of corner and edge sites found on smaller crystallites.[22]

Carbon monoxide adsorbs on SBA-15 at room temperature and desorbs slowly under vacuum or He purge. Peaks at ∼2003 and 2028 cm^{-1} are associated with CO adsorbed to SBA-15 (Figure 1A). Both peaks lose significant intensity upon heating, and at a temperature of >353 K, both bands disappear. These peaks are significantly red-shifted relative to CO hydrogen-bonded to silanol groups at low temperatures (2158 and 2140 cm^{-1}) or gas-phase CO (2143 cm^{-1}).[23] No reports of CO stretching frequencies reduced by this amount on silica could be found in the literature. Adsorption of CO on ultrapure SBA-15[24] produced the same bands, and therefore, the adsorption of CO is not attributed to transition metal contamination.

3.2. Volumetric Adsorption and IR Spectroscopy of CO and C_2H_4 Adsorption on Clean Pt/SBA-15. The volumetric adsorption uptakes for CO and C_2H_4 on clean Pt surfaces are compiled in Table 2. Both total and irreversible CO uptakes decreased at 403 K, while the amount of reversibly adsorbed CO was similar. Comparison of irreversible uptakes at the two temperatures demonstrated that chemisorption decreased by 20−35% on the Pt/SiO_2 catalysts, 20% on Pt powder, and ∼50% on the Pt/Al_2O_3 catalyst at the higher temperature.

The IR spectroscopy of CO adsorbed to solid surfaces is a qualitative probe of surface structure due to the sensitivity of ν(CO) to the structure of the metal atom(s) to which it is coordinated.[25] Diffuse-reflectance infrared spectra (1900−2100 cm^{-1}) of CO adsorbed on the series of SBA-15 supported Pt catalysts are shown in Figure 1.[9] Spectra B−E are CO adsorbed to Pt on a series of Pt/SBA-15 samples at room temperature after subtraction of the CO−SBA-15 interaction. Linear-bound CO was the only surface CO species identified on all samples; μ_2 and μ_3 modes of CO were not detected. Spectra F−H demonstrate that linear-bound CO was the only adsorbed species on the atomically dispersed 3.2% Pt/SiO_2, while the CO peak position on the alumina support was red-shifted by 10 cm^{-1} compared to a Pt/SiO_2 catalyst with a similar particle size. The influence of temperature on the band position of linearly adsorbed CO for the 2.69% Pt(2.9 nm)/SBA-15 catalyst is shown in Figure 2A and B. If it is assumed that the intensity of the IR band is proportional to the amount of CO species on the surface and the IR extinction coefficient is independent of the adsorption temperature, then the relative coverage is obtained by the ratio of the IR band intensity at a temperature to the band intensity for CO adsorption after exposure to 76 Torr CO at room temperature.[26,27] Using this approach, the relative coverage of CO at 403 K is estimated to be ∼0.7 (Figure 2C), and only above ∼380 K does the coverage of CO begin to decrease.

The volumetric adsorption of ethylene on supported Pt catalysts has been studied to a lesser extent.[28] At adsorption temperatures of 298 and 403 K, in the absence of H_2, most of the adsorbed ethylene is assumed to convert to ethylidyne. The strong intermolecular repulsion between ethylidyne limits the coverage on Pt surfaces to 0.25 ML.[29] Total uptakes are greater at 403 K than at 298 K for all samples (except for Pt/Al_2O_3). The increased total adsorption is split between irreversible and reversible adsorption for most catalysts. The C_2H_4/Pt_s adsorption stoichiometries are all <1 and increase with temperature. The ratio Pt_s/C_2H_4 (Table 3) is an indication of the number of sites required to convert adsorbed C_2H_4 to ethylidyne, and it is both particle size and temperature-dependent. Adsorption and decomposition of ethylene at 298 K requires 2−7 atoms with the number of

(23) Beebe, T. P.; Gelin, P.; Yates, J. T. *Surf. Sci.* **1984**, *148*, 526.
(24) Ultrapure SBA-15 was synthesized according to the literature,[10] but the reagents used were 99.999% TEOS, 20% doubly-distilled HCl, and ultrapure H_2O.
(25) Hofmann, F. M. *Surf. Sci. Rep.* **1983**, *3*, 107.
(26) Bourane, A.; Dulaurent, O.; Bianchi, D. *J. Catal.* **2000**, *196*, 115.
(27) Bourane, A.; Dulaurent, O.; Chandes, K.; Bianchi, D. *Appl. Catal. A: Gen.* **2001**, *214*, 193.
(28) Passos, F. B.; Schmal, M.; Vannice, M. A. *J. Catal.* **1996**, *160*, 118.
(29) Starke, U.; Barbieri, A.; Materer, N.; Hove, M. A. V.; Somorjai, G. A. *Surf. Sci.* **1993**, *286*, 1.

Table 2. Sequential Co-adsorption Uptakes of Carbon Monoxide and Ethylene on Supported Pt Catalysts at 298 and 403 K

	CO uptake on clean Pt surface[a,b]				C_2H_4 uptake on clean Pt surface[a,b]			
	CO at 298 K		CO at 403 K		C_2H_4 at 298 K[c]		C_2H_4 at 403 K[c]	
catalyst	total	irrev	total	irrev	total	irrev	total	irrev
2% Pt/Al_2O_3 (Exxon)	80.6	70.1	44.6	34.5	30.5	16.0	29.2	24.6
3.2% Pt/SiO_2-IE	166.7	152.2	138.5	110.3	57.0	51.0	74.1	67.0
2.33% Pt(1.7 nm)/SBA-15	66.1	59.6	52.4	46.5	25.5	22.9	40.1	29.4
2.69% Pt(2.9 nm)/SBA-15	39.5	34.9	32.6	26.1	14.4	11.9	22.5	16.4
2.62% Pt(3.6 nm)/SBA-15	32.8	30.7	27.6	19.8	13.1	10.1	17.6	12.9
2.86% Pt(7.1 nm)/SBA-15	14.7	11.7	9.5	7.9	6.9	4.9	7.5	5.6
UHP Pt powder	15.1	13.7	12.9	10.2	3.6	2.9	5.0	4.2
	CO uptake on an ethylene-covered Pt surface[a]				C_2H_4 uptake on "CO-covered" surface[a,b]			
	CO at 298 K		CO at 403 K		C_2H_4 at 298 K		C_2H_4 at 403 K	
catalyst	total	irrev	total	irrev	total	irrev	total	irrev
2% Pt/Al_2O_3 (Exxon)	17.2	12.1	32.6	22.1	18.7	0.4	12.4	5.5
3.2% Pt/SiO_2-IE	78.9	72.4	98.5	67.5	4.8	0.0	16.5	3.4
2.33% Pt(1.7 nm)/SBA-15	32.8	29.5	39.3	29.2	1.9	0.1	9.2	1.7
2.69% Pt(2.9 nm)/SBA-15	17.4	13.2	21.5	14.1	1.6	0.2	5.0	1.1
2.62% Pt(3.6 nm)/SBA-15	14.1	11.4	19.1	10.9	1.1	0.0	3.7	0.6
2.86% Pt(7.1 nm)/SBA-15	5.1	3.1	7.8	2.4	0.5	0.0	1.7	0.3
UHP Pt powder	8.5	7.9	7.2	4.8	0.2	0.07	1.4	0.4

[a] Uptakes extrapolated to zero pressure (monolayer uptake). [b] Uptakes in μmol g^{-1}.

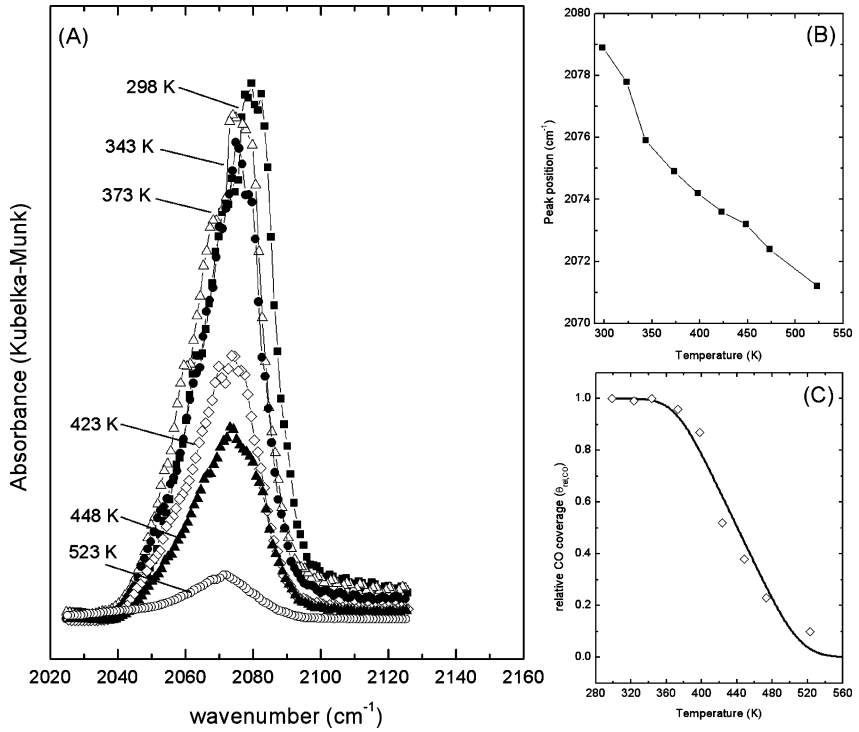

Figure 2. (A) Temperature dependence of linear-bound CO position for 2.69% Pt(2.9 nm)/SBA-15. (B) Peak position of linear-bound CO as a function of temperature. (C) Temperature dependence of CO coverage on the 2.69% Pt(2.9 nm)/SBA-15 catalyst. The integrated intensity of the CO band was used to calculate the relative coverage. The solid line represents a fit of the Temkin adsorption model assuming heats of adsorption of 40 kcal mol^{-1} ($\theta_{CO} = 0$, initial) and 30 kcal mol^{-1} ($\theta_{CO} = 1$, saturation).

atoms increasing with particle size. The required number of sites decreases to 2−5 at 403 K. Both sets of numbers are in good agreement with work on Pt(111), which suggested that an ensemble size of four atoms is necessary for ethylene adsorption.[30]

Infrared studies of C_2H_4 adsorption on supported Pt catalysts have been performed in an attempt to determine the type and concentration of ethylene-derived intermediates[31,32] and the influence of particle size on C_2H_4 adsorption and decomposition. Figure 3 shows DRIFTS spectra of C_2H_4 adsorbed on different Pt catalysts at 298 K. No stable IR-active surface species were identified on pure SBA-15 silica upon exposure to C_2H_4. The adsorption of ethylene to Pt/SBA-15 gave rise to spectroscopic

(30) Windham, R. G.; Koel, B. E.; Paffett, M. T. *Langmuir* **1988**, *4*, 1113.

(31) Mohsin, S. B.; Trenary, M.; Robota, H. J. *J. Phys. Chem.* **1988**, *92*, 5229.

(32) Mohsin, S. B.; Trenary, M.; Robota, H. J. *Chem. Phys. Lett.* **1989**, *154*, 511.

Table 3. Surface Pt (Pt_s)/C_2H_4 Stoichiometry Determined for a Clean Pt Surface Based on Volumetric Adsorption Uptakes at 298 and 403 K

	Pt_s/C_2H_4 stoichiometry[a]	
catalyst	298 K	403 K
2% Pt/Al_2O_3 (Exxon)	2.8	1.8
3.2% Pt/SiO_2-IE	3.2	2.4
2.33% Pt(1.7 nm)/SBA-15	2.8	2.2
2.69% Pt(2.9 nm)/SBA-15	4.3	3.1
2.62% Pt(3.6 nm)/SBA-15	3.5	2.7
2.86% Pt(7.1 nm)/SBA-15	3.9	3.4
UHP Pt powder	7.1	4.9

[a] Surface platinum based on total H_2-O_2 titration at 298 K.

features at ~1340, ~1420, and ~1500 cm^{-1} assigned to ethylidyne (methyl symmetric deformation ($\delta_s(CH_3)$), di-σ-bonded ethylene (methylene symmetric deformation ($\delta_s(CH_2)$), and π-bonded ethylene (ν(C═C) and $\delta(CH_2)$ normal modes), respectively.[33] The ratio of these surface species is highly dependent on the Pt particle size. According to DRIFTS data, samples with Pt particles of ≤2 nm exposed to C_2H_4 have a ratio of ethylidyne/π-bonded ethylene/di-σ-bonded ethylene of ~1:1:1. The IR spectra of samples with Pt particles larger than 2 nm were dominated by ethylidyne. The moderately weak C−C stretch in ethylidyne has been identified at 1126 cm^{-1} on Pt(111), but it is not detectable on SBA-15 catalysts due to strong SiO_2 absorption bands in this region. Upon the introduction of 5 Torr H_2 to the evacuated DRIFTS cell at room temperature, all ethylene-derived surface species were removed from the surface. Ethylidyne was the only observed spectral feature upon adsorption of C_2H_4 at 403 K (infrared spectrum not shown). It is postulated that, on a clean Pt surface at 403 K, π-bonded ethylene has desorbed or converted to di-σ-bonded ethylene, which is subsequently converted to ethylidyne.[34,35]

3.3. Volumetric Adsorption and IR Spectroscopy of CO and C_2H_4 Sequential Co-adsorption on Clean Pt/SBA-15. The data from sequential uptakes of C_2H_4 and CO on the Pt/SBA-15 catalysts and Pt powder are compiled in Table 2. Examples of sequential CO and C_2H_4 adsorption isotherms at 298 and 403 K are given in Figure 4. Chemisorption of CO on an ethylene-covered surface results in a substantial decrease of the amount of CO adsorbed/Pt(s) compared to a clean Pt surface. On Pt/silica catalysts, irreversible CO uptakes decreased 42−74% and 37−70% at 298 and 403 K, respectively, upon adsorption onto a C_2H_3-covered surface. The amount of reversibly adsorbed CO on the ethylidyne-covered surface was similar at both temperatures. Reversing the adsorption sequence, it is evident that CO is much more effective at excluding C_2H_4 from the surface. At 298 and 403 K, irreversible C_2H_4 adsorption on a CO-covered surface is effectively quenched (irreversible C_2H_4 uptakes decreased >98% and >90%, respectively).

The vibrational spectrum of a 2.69% Pt(2.9 nm)/SBA-15 catalyst exposed to C_2H_4 after removal of gas-phase C_2H_4 by He purge at 298 K is shown in Figure 5A. The observed vibrational bands are assigned to π-bonded ethylene (1499 cm^{-1}), di-σ-bonded ethylene (1421 cm^{-1}), and ethylidyne (1345 cm^{-1}) and are in agreement with spectroscopic data obtained upon ethylene adsorption on a clean Pt surface.[31] The vibrational features of ethylene-derived adsorbates after CO exposure to an ethylene-covered surface are shown in Figure 5B. The band at ~1500 cm^{-1}, attributed to π-bonded ethylene, has lost significant intensity, and the amount of di-σ-bonded ethylene has also decreased. A band at 2050 cm^{-1} for adsorbed carbon monoxide appears in the spectrum, which is red-shifted compared to that of CO adsorbed to a clean Pt surface (see Figure 1C). Upon heating to 403 K under a He purge, the ethylidyne band is slightly reduced in intensity and red-shifted to 1340 cm^{-1} (Figure 5C). Minimal changes occur in the vibrational spectrum upon heating (compare 5B and C); exhibiting behavior consistent with C_2H_3 on Pt. Additional heating to 500 K led to a decrease in the ethylidyne and CO vibrational bands due to decomposition and desorption, respectively.

4. Discussion

4.1. Infrared Spectroscopy of Carbon Monoxide Adsorption on Clean Pt Surfaces. Carbon monoxide is an ideal probe of heterogeneous adsorption kinetics and dynamics because of its sensitivity to the local environment, both the underlying metal structure and neighboring adsorbates.[25] The bonding of CO to the metal surface occurs through donation of electron density in the 5σ orbital of CO to unoccupied metal orbitals and back-donation of electron density from the filled surface d-band of the metal to unoccupied 2π* orbitals on CO.[36] The degree of back-donation is related to the availability of electron density on the metal and the energy match between the surface d-band of the metal with the 2π* orbitals on CO. Using a plane-wave basis to model the valence electrons on Pt surfaces, Hammer et al. calculated the density of states at selected adsorption sites. A significant shift of the d-band center is apparent upon comparison of Pt surface sites (ϵ = d-band center, E_F = Fermi level): Pt(100), $\epsilon - E_F = -3.0$ eV; Pt(111), $\epsilon - E_F = -2.8$ eV; Pt(211) step, $\epsilon - E_F = -2.4$ eV; Pt(11 8 5) kink, $\epsilon - E_F = -2.0$ eV.[37] The calculated data indicate better availability of the metal electron density on rough surfaces, since the energy match with 2π* CO orbitals improves as the d-band center shifts toward the Fermi level. The theoretical predictions are pertinent to complex 3D catalysts, such as Pt/SiO_2, since stepped single-crystal surfaces can serve as models for small catalyst particles.[38,39] Crystallites possess face, edge, and corner sites that exist on the surface in a specific ratio, dependent on the diameter of the particle.[22] At low coverage, CO selectively adsorbs on the edges and kinked edges of Pt(533) and Pt(432) single crystals, giving rise to ν(CO) = 2065 cm^{-1} (no difference within ±2 cm^{-1}). At saturation coverage, CO binds in the linear-bound mode to the (111) terraces of Pt(533), and ν(CO) = 2097 cm^{-1}.[38]

4.2. Influence of Temperature on CO Adsorption. The peak position of the linear-bound CO in the temperature range 298−523 K is shown in Figure 2B. In the present study, ν(CO) red-shifts with increasing temperature; typical values of $\Delta\nu$(CO) = 8−9 cm^{-1}. The change in ν(CO) with increasing temperature is small compared to changes in frequency due to coverage effects and increased dipole−dipole coupling.[40,41] The temperature dependence of ν(CO) could be a result of the dependence of ν(CO) on coverage effects, since desorption of CO occurs at elevated temperatures. The CO molecule is a π-electron acceptor when the molecule binds to electron-rich metals. Given that fewer CO molecules reside on the metal surface at higher temperature,

(33) Spiewak, B. E.; Cortright, R. D.; Dumesic, J. A. *J. Catal.* **1998**, *176*, 405.
(34) Erley, W.; Li, Y.; Land, D. P.; Hemminger, J. C. *Surf. Sci.* **1994**, *301*, 177.
(35) Land, T. A.; Michely, T.; Behm, R. J.; Hemminger, J. C.; Comsa, G. *J. Chem. Phys.* **1992**, *97*, 6774.
(36) Blyholder, G. *J. Phys. Chem.* **1964**, *68*, 2772.
(37) Hammer, B.; Nielsen, O. H.; Nørskov, J. K. *Catal. Lett.* **1997**, *46*, 31.
(38) Greenler, R. G.; Burch, K. D.; Kretzschmar, K.; Klauser, R.; Bradshaw, A. M.; Hayden, B. E. *Surf. Sci.* **1985**, *152*, 338.
(39) Hayden, B. E.; Kretzschmar, K.; Bradshaw, A. M.; Greenler, R. G. *Surf. Sci.* **1985**, *149*, 394.
(40) Eischens, R. P.; Francis, S. A. *J. Phys. Chem.* **1956**, *60*, 194.
(41) Klünker, C.; Balden, M.; Lehwald, S.; Daum, W. *Surf. Sci.* **1996**, *360*, 104.

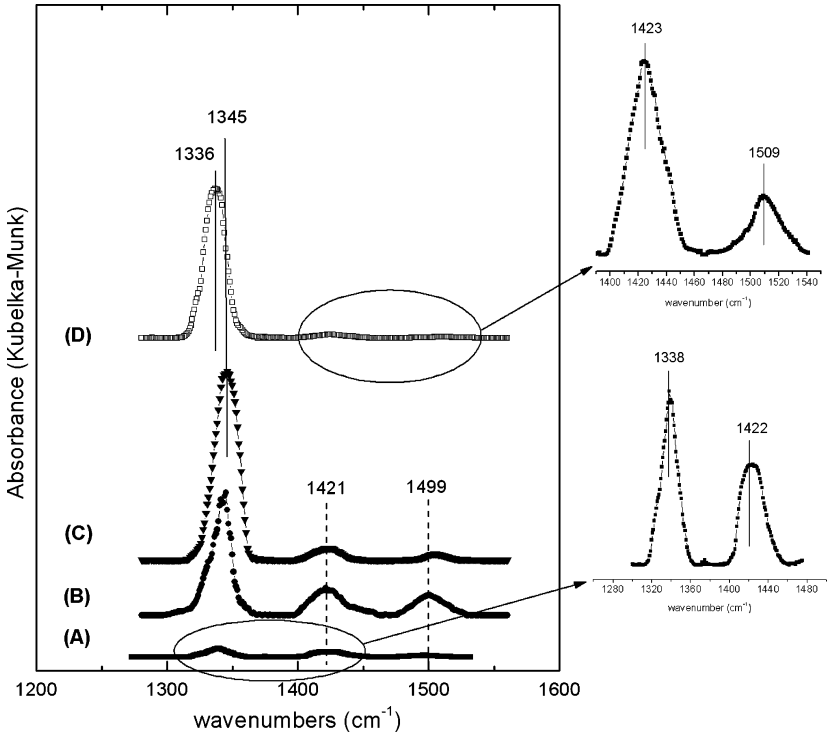

Figure 3. Diffuse-reflectance infrared spectra of C_2H_4 adsorbed at 300 K on Pt(*X*)/SBA-15: (A) 1.7 nm, (B) 2.9 nm, (C) 3.6 nm, and (D) 7.1 nm particles.

there is less competition for the same available electron density on the metal surface, which in turn results in better back-donation to the ligand. It should be noted, however, that a red-shifted peak (CO−Pt(step), ν(CO) = 2065 cm^{-1}) does not appear at higher temperature;[39] thus, the data appear to indicate high CO coverage on Pt at 523 K. To reconcile the fact that edge site CO was not observed while the absorption intensity of the CO stretch decreases at high temperature, we propose that CO dissociates on the surface to form carbonaceous deposits on the step edge sites.[42,43]

The relative CO coverage could be quantified (assuming that the surface was saturated under room-temperature conditions) according to the integrated peak areas from the temperature-dependent IR data. The outcome of this calculation is shown in Figure 2C. The solid line fit to the data is a Temkin adsorption model assuming an initial heat of adsorption $\Delta H_{ads}(\theta = 0)$ of 40 kcal mol^{-1} and ΔH_{ads} at saturation of 30 kcal mol^{-1}. Previous work on close-packed Pt single-crystal surfaces have shown that CO adsorption isotherms can be described by the Temkin model.[44] As discussed below, the ΔH_{ads} values are on the higher end of the experimentally reported values, but they adequately fit the data and demonstrate that CO desorption from a 2.9 nm particle surface does not begin until ∼380 K. As the coverage increases, intermolecular interactions become repulsive and the heat of adsorption decreases in a linear fashion according to the Temkin model. An initial differential heat of adsorption of CO at 403 K has been measured on a 0.85% Pt/SiO_2 catalyst as 33 kcal mol^{-1}, which decreases to 9.5 kcal mol^{-1} at saturation coverage.[45,46] CO saturates the Pt particle surface at a coverage of 0.68 ML on Pt(111) as determined by scanning tunneling microscopy (STM),[21,47] and a ΔH_{ads} value of 10 kcal mol^{-1} has been determined by laser induced thermal desorption (LITD)[48] at these conditions.

4.3. Influence of Pt Particle Size on CO Adsorption. The heat of adsorption of CO is dependent on the supported Pt crystallite size, with smaller particles showing slightly higher heats of adsorption.[49] The reported heats of adsorption from temperature-programmed desorption (TPD) studies of CO at low coverages were dependent upon Pt surface structure and varied from 28 kcal mol^{-1} for the Pt(110)-(2 × 1) surface to 34 kcal mol^{-1} for the Pt(210) surface.[44] The heats of adsorption from the three most stable surfaces of Pt (i.e., (100), (111), and (110)) were 27−29 kcal mol^{-1}.[6] This suggests that the heat of adsorption does not vary significantly as a function of surface structure but does demonstrate that CO should bind to defect sites before terrace atoms. In fact, it has been shown that CO molecules adsorb at step edges first to form a 1D chain, and only after the step is saturated will CO molecules adsorb to terrace sites beginning with those adjacent to the step edge.[50] This adsorption sequence (step then terrace atoms) was shown to be dominant on Pt(211)[51] but not on Pt(311),[52] suggesting that the CO−surface interaction is not dictated by thermodynamics alone.

DRIFTS data for Pt/SBA-15 samples exposed to CO are shown in Figure 6. Within a size range of 1.9−7.1 nm, ν(CO) shifts 15 cm^{-1}, exhibiting a continuous red-shift as particle size decreases. Kappers and van der Maas[53] found a linear correlation between the Pt coordination number and ν(CO) for a series of Pt supported catalysts with varying particle sizes. Cant and Donaldson[54] have

(42) Kung, K. Y.; Chen, P.; Wei, F.; Shen, Y. R.; Somorjai, G. A. *Surf. Sci.* **2000**, *463*, L627.
(43) McCrea, K.; Parker, J. S.; Chen, P.; Somorjai, G. A. *Surf. Sci.* **2001**, *494*, 238.
(44) McCabe, R. W.; Schmidt, L. D. *Surf. Sci.* **1977**, *66*, 101.
(45) Sen, B.; Vannice, M. A. *J. Catal.* **1991**, *130*, 9.
(46) Vannice, M. A.; Hasselbring, L. C.; Sen, B. *J. Catal.* **1986**, *97*, 66.
(47) Longwitz, S. R.; Schnadt, J.; Vestergaard, E. K.; Vang, R. T.; Lægsgaard, E.; Stensgaard, I.; Brune, H.; Besenbacher, F. *J. Phys. Chem. B* **2004**, *108*, 14497.
(48) Seebauer, E. G.; Kong, A. C. F.; Schmidt, L. D. *Surf. Sci.* **1986**, *176*, 134.
(49) Rogozik, J.; Dose, V. *Surf. Sci.* **1986**, *176*, L847.
(50) Lambert, D. K. *Phys. Rev. Lett.* **1983**, *50*, 2106.
(51) Brown, W. A.; Kose, R.; King, D. A. *Surf. Sci.* **1999**, *440*, 271.
(52) Kose, R.; King, D. A. *Chem. Phys. Lett.* **1999**, *313*, 1.
(53) Kappers, M. J.; van der Maas, J. H. *Catal. Lett.* **1991**, *10*, 365.
(54) Cant, N. W.; Donaldson, R. A. *J. Catal.* **1982**, *78*, 461.

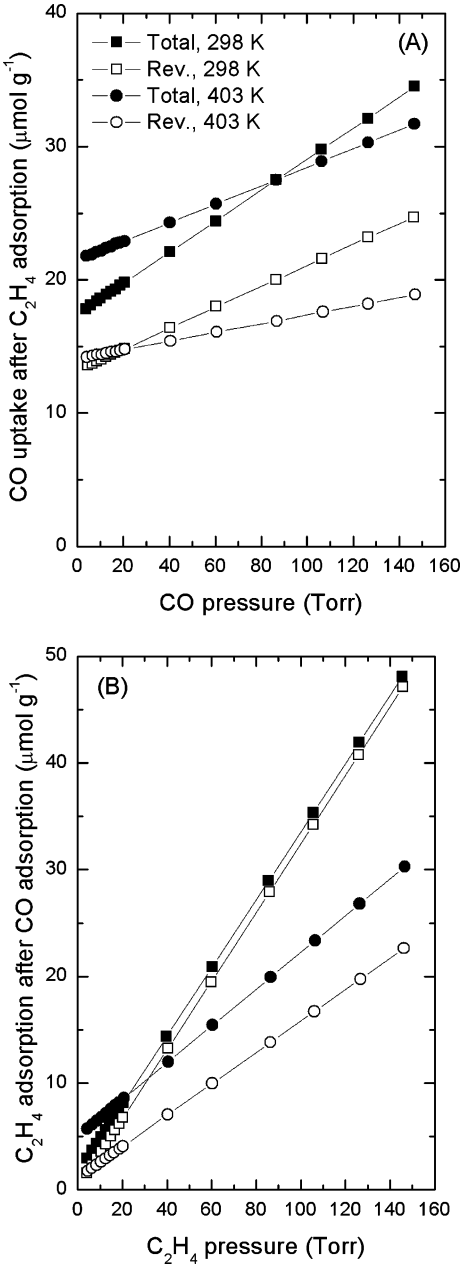

Figure 4. Sequential CO and C_2H_4 adsorption experiments on 2.69% Pt(2.9 nm)/SBA-15: (A) CO adsorption on a C_2H_4-covered surface at 298 and 403 K and (B) C_2H_4 adsorption on a CO-covered surface at 298 and 403 K.

shown a minor influence of particle size on the position of the linear-bound CO vibration for two Pt/SiO_2 catalysts with particle sizes determined by chemisorption of 1.8 and 18 nm; the band position for the 1.8 nm was red-shifted by 6 cm^{-1} relative to the 18 nm Pt particle silica catalyst (2078 cm^{-1}). Bischoff and co-workers[55] have studied the effect of particle size on CO adsorption for Pt dispersed within a neutralized faujasite zeolite; a clear particle size dependent shift of the linear-bound CO stretching vibration was observed due to the narrow Pt particle size distribution. At room temperature, the linear-bound CO stretching frequency was ∼2050 cm^{-1} for 1−2 nm particles and ∼2100 cm^{-1} for 4−5 nm particles. Clearly, work on single crystals[43,56] and supported catalysts[54,55] suggests that the position of the linear-bound CO vibration red-shifts with increasing surface roughness

(55) Bischoff, H.; Jaeger, N. I.; Schulz-Ekloff, G. *Z. Phys. Chem. (Leipzig)* **1990**, *271*, 1093.

(56) Mukerji, R. J.; Bolina, A. S.; Brown, W. A. *Surf. Sci.* **2003**, *527*, 198.

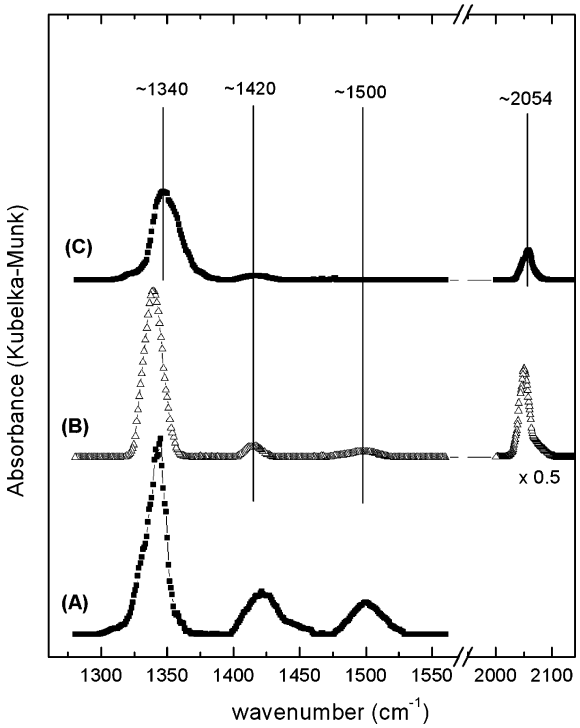

Figure 5. Diffuse-reflectance infrared spectra of (A) adsorbed C_2H_4 on a clean Pt surface after He purging, (B) a Pt surface after introduction of 76 Torr CO to an ethylene-covered surface and He purge at 298 K, and (C) a Pt surface with co-adsorbed CO and C_2H_3 after He purge at 403 K. All adsorption experiments were conducted on a 2.69% Pt(2.9 nm)/SBA-15 catalyst.

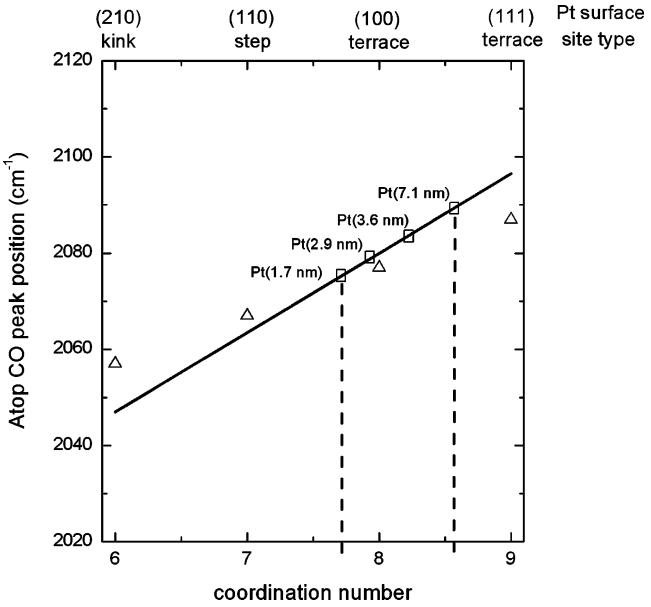

Figure 6. Influence of Pt coordination number on the peak position of the linear-bound CO for the Pt/SBA-15 catalyst series. Fitting the data from the Pt/SBA-15 series to a previously proposed relationship[53] between the peak position of the linear-bound CO and the Pt coordination number, the average coordination number is 7−9, indicating adsorption on defect and terrace sites. Triangles are singleton CO frequencies as a function of Pt atom coordination.[62] The Pt surface structure and site type are given as an example of an entity with the corresponding coordination number.

and decreasing particle size. The stretching frequency of a single CO molecule (singleton) on a Pt_{10} cluster determined by density functional theory (DFT) calculations is 2050 cm^{-1},[57] while a single CO stretching vibrational frequency of 2020 cm^{-1} was

Scheme 1. Ethylene-Derived Surface Species on Pt: (A) π-Bonded Ethylene; (B) Di-σ-bonded Ethylene; (C) Ethylidyne; and (D) Ethan-1-yl-2-ylidyne

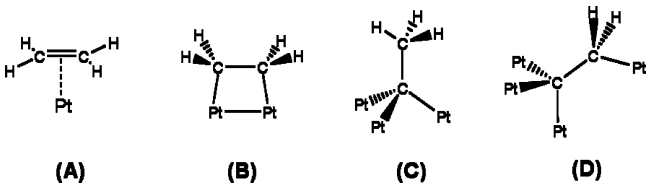

reported for a neutral gas-phase $Pt_3(CO)_6$ clusters.[58] Vibrational frequencies for linear-bound CO have been reported at 2000 cm^{-1} for $Pt(CO)_2$-type surface species,[59] and frequencies as low as 1990 cm^{-1} have been reported for CO molecules adsorbed on step sites of 6−8 Pt atom clusters inside zeolite L channels.[60]

The molecular orbital picture of CO bonding to transition metal surfaces was proposed by Blyholder[36] and has been confirmed by density functional methods.[57,61] The work presented here is in agreement with previous studies and suggests that the degree of π back-donation to CO is stronger on a small particle with a larger fraction of low coordination metal sites than on a single crystal or platinum particle with a large fraction of high coordination surface sites.[59] Pt−carbonyl cluster studies have shown that the strength of π back-bonding of the CO chemisorption bond to a small particle is stronger than to a surface.[59]

All CO spectra on the Pt/SBA-15 catalysts consist of a single absorption peak, although some particle sizes have a small shoulder to the red of the maximum (Figure 1). Previous experimental and modeling work on small Pt crystallites produced complex CO spectra with multiple peaks, indicative of CO bonding to surface atoms with different coordination and complex phase interactions between neighboring adsorbates. For example, four CO species have been identified during the low temperature adsorption of CO on a stepped Pt(211) single crystal.[56] The situation is potentially more complex on a Pt nanoparticle due to surface roughness. IR spectra of CO adsorbed on 39 Å particles were much more complex than spectra of CO on 11 Å particles.[62] Based on low coverage experimental studies on Pt and on a coupled harmonic oscillator model,[63] CO vibrations at 2070, 2080, and 2090 cm^{-1} are due to CO located at edges, terrace (100) atoms, and terrace (111) atoms, respectively.

4.4. Ethylene Adsorption on Pt Catalysts: Influence of Particle Size. Ethylene adsorbs molecularly on Pt(111) at low temperatures (≤200 K), forming up to three species: π-, di-σ-bonded, or ethylidyne (Scheme 1). The heat of adsorption of π-bonded ethylene on clean Pt(111) was measured as 9.6 kcal mol^{-1}.[64] Co-adsorption of Bi atoms and ethylene suggest that an ensemble size of four atoms is necessary for ethylene adsorption on Pt(111).[65] The type of ethylene bound species is dependent upon metal surface and temperature; Stuve and Madix[66] have introduced the $\pi\sigma$ parameter, which is a measure of the degree of π to di-σ character. It has been shown on Pt(111) that di-σ-bonded ethylene is favored and has a $\pi\sigma$ parameter of 0.92, while for Pd(100) the same parameter has a value of 0.37, favoring π-bonded ethylene.[67] The di-σ ethylene dehydrogenates to form an intermediate with C_3 symmetry. The intermediate was first proposed to be ethylidene[68] but later shown to be ethylidyne, which binds with its CC axis perpendicular to the surface. LEED studies have shown that ethylidyne adsorbs in face-centered cubic (fcc) 3-fold hollow sites on a Pt(111) surface[29] and is stable up to 430−450 K. Above these temperatures, ethylidyne decomposes either to CH_x fragments or to adsorbed carbon and hydrogen atoms and forms carbon particles of up to ∼30−40 atoms.[35]

Most low- and high-pressure surface science studies have been performed on Pt(111), but the surface chemistry of ethylene has been studied on other Pt single crystals. Notably, characterization of the influence of surface structure has been undertaken by Masel and co-workers.[69−73] The activation energy for the desorption of ethylene (θ = 0.1−0.25) from Pt surfaces with varying step atom density varied from 12 to 19 kcal mol^{-1}. A correlation between step atom density and self-hydrogenation was found to be dependent on the concentration of π-bonded ethylene on step sites. Surfaces with intermediate step atom densities converted ethylene to methane under UHV conditions.[74] The (1 × 1) Pt(110)[70] and (2 × 1) Pt(110)[71] surfaces were very active for carbon−carbon bond scission and coke formation. On the (1 × 1) Pt(110) surface, π-bonded ethylene forms at 93 K. This is contrary to previous results on Pt(111), (5 × 20) Pt(100) (pseudohexagonal), or (1 × 1) Pt(100) surfaces where di-σ-bonded ethylene was identified at the same conditions,[70] but is in agreement with theory which predicts that (1 × 1) Pt(110) has one of the highest orbital availabilities for the formation of π-bonded ethylene. The π-bonded form converted to di-σ-bonded ethylene upon heating to 220 K, and at 300 K ethane and methane evolved from the surface. No formation of ethylidyne has been observed on (1 × 1) Pt(100),[70] but rather a vinylidene intermediate has been proposed. Ethylidyne formation has been observed by high-resolution electron energy loss spectroscopy (HREELS) on (2 × 1) Pt(110), and it has been proposed that ethylidyne forms in the valleys of the (2 × 1) structure by a mechanism identical to one proposed for Pt(111).[75] By 400 K, H_2 TPD and HREELS spectra are complex and suggest that a mixture of C_2 species, denoted as $[-C\equiv C-]_x$, accumulates on the surface with adsorbed atomic carbon. These species have also been observed on the (2 × 1) Pt(110) surface.[72]

The π-bonded ethylene species most readily forms, and most effectively stabilized, on the Pt(210) surface.[69] The highly stepped nature of the (210) surface enables π-bonded ethylene to form on step sites, while di-σ formation is sterically hindered. The π-species is stable up to 300 K on the Pt(210) surface, in contrast to the (1 × 1) Pt(110) surface where its intensity is attenuated after annealing to 160 K. The IR bands associated with π-bonded ethylene are attenuated on (2 × 1) Pt(110) at 100 K. No ethylidyne has been observed on Pt(210) upon heating due to the highly strained nature of a CCH_3 species on this surface. There is not enough space for ethylidyne to stand up over the fcc 3-fold

(57) Watwe, R. M.; Spiewak, B. E.; Cortright, R. D.; Dumesic, J. A. *Catal. Lett.* **1998**, *51*, 139.
(58) Icking-Konert, G. S.; Handschuh, H.; Ganteför, G.; Eberhardt, W. *Phys. Rev. Lett.* **1996**, *76*, 1047.
(59) Härle, H.; Metka, U.; Volpp, H. R.; Wolfrum, J. *Phys. Chem. Chem. Phys.* **1999**, *1*, 5059.
(60) Lane, G. S.; Miller, J. T.; Modica, F. S.; Barr, M. K. *J. Catal.* **1993**, *141*, 465.
(61) Feibelman, P. J.; Hammer, B.; Nørskov, J. K.; Wagner, F.; Scheffler, M.; Stumpf, R.; Watwe, R.; Dumesic, J. *J. Phys. Chem. B* **2001**, *105*, 4018.
(62) Brandt, R. K.; Hughes, M. R.; Bourget, L. P.; Truszkowska, K.; Greenler, R. G. *Surf. Sci.* **1993**, *286*, 15.
(63) Brandt, R. K.; Sorbello, R. S.; Greenler, R. G. *Surf. Sci.* **1992**, *271*, 605.
(64) Kubota, J.; Ichihara, S.; Kondo, J. N.; Domen, K.; Hirose, C. *Surf. Sci.* **1996**, *358*, 634.
(65) Campbell, C. T.; Campbell, J. M.; Dalton, P. J.; Henn, F. C.; Rodriguez, J. A.; Seimanides, S. G. *J. Phys. Chem.* **1989**, *93*, 806.
(66) Stuve, E. M.; Madix, R. J. *J. Phys. Chem.* **1985**, *89*, 3183.
(67) Stuve, E. M.; Madix, R. J. *J. Phys. Chem.* **1985**, *89*, 105.
(68) Ibach, H.; Lehwald, S. *J. Vac. Sci. Technol.* **1978**, *15*, 407.
(69) Blackman, A. L.; Masel, R. I. *J. Phys. Chem.* **1990**, *94*, 5300.
(70) Hatzikos, G. H.; Masel, R. I. *Surf. Sci.* **1987**, *185*, 479.
(71) Yagasaki, E.; Blackman, A. L.; Masel, R. I. *J. Phys. Chem.* **1990**, *94*, 1066.
(72) Yagasaki, E.; Masel, R. I. *Surf. Sci.* **1989**, *222*, 430.
(73) Yagasaki, E.; Masel, R. I. *Surf. Sci.* **1990**, *226*, 51.
(74) Yagasaki, E.; Masel, R. I. *J. Am. Chem. Soc.* **1990**, *112*, 8746.
(75) Zaera, F. *J. Am. Chem. Soc.* **1989**, *111*, 4240.

hollow site due to the steric influence of the opposing step. Rather, the authors suggest that an ethan-1-yl-2-ylidyne ($\equiv CCH_2-$) species forms (Scheme 1). This species is likely present on (1 × 1) Pt(110) and (2 × 1) Pt(110) during ethylene decomposition (Pt(210) and (1 × 1) Pt(110) have a similar step geometry). The same species is thought to bond to three step atoms and one terrace atom on the reconstructed (1 × 2) Pt(311) surface.[51]

Few studies are available that provide data on the influence of particle size on the formation and stability of ethylene-derived species. In this study, ethylidyne forms upon adsorption on particles, as well as π- and di-σ-bonded ethylene, but in different proportions depending on crystallite size. Very little ethylidyne was formed on the 1.7 nm crystallites, while its formation on 2.9, 3.6, and 7.1 nm crystallites was substantially larger. Both di-σ- and π-bonded ethylene was found in high concentrations on the 2.9 nm surface. Over a series of Pt/Al_2O_3 catalysts with varying dispersion, ethylidyne was favored relative to π-bonded ethylene as particle size increases.[31] This suggests that undercoordinated sites are primarily responsible for the formation of π-bonded ethylene, which is in agreement with the stability of π-bonded ethylene on step edges of Pt(210).[76] Vibrational coupling of adsorbed $^{13}C_2H_4/^{12}C_2H_4$ shows that ethylidyne is produced on (111) facets of Pt particles ($d = 10-40$ Å, avg. $= 20$ Å) rather than on random trimer Pt sites.[77] No ethylidyne was detected on sub-nanometer Pt particles ($d \leq 10$ Å). Beebe and Yates[78] have suggested that the inability of ethylidyne to form on surfaces lacking 3-fold symmetry makes it a useful probe to determine the fraction of (111) oriented surfaces. Ethylene adsorption at 300 K led to the formation of ethylidyne on Pt crystallites of 2.2 nm, which were thought to consist primarily of (111) facets with a small fraction of (100) surfaces.[79] The stability of π-bonded ethylene on Pt catalysts prepared by chloride impregnation[31] was greater than that found by Masel and co-workers on Pt(210) and Pt/SiO_2 catalysts. Passos et al.[28] found that the initial heat of adsorption at 300 K was 10 kcal mol^{-1} higher on large (∼20 nm) Pt particles as compared with small Pt particles (∼1 nm); the higher heat of adsorption on large crystallites was attributed to the exothermic dehydrogenation of ethylene to ethylidyne.[80] Correction of reported TPD data for the enthalpy of reaction for the dehydrogenation of ethylene to ethylidyne yields ethylene heat of adsorption values on Pt single crystals which are similar to values measured on large (≥4 nm) Pt crystallites.[28,81]

It is clear from our spectroscopic data that the fraction of π-bonded ethylene is vastly higher on the 1.7 nm Pt particles and decreases with increasing particle size. The increased abundance of π-bonded ethylene on the surface of small particles is consistent with the idea that these surfaces are rough. The surface of the 1.7 nm Pt particles have a higher ratio of corner and edge surface atoms, which stabilize the π-bonded ethylene, presumably in the same manner as the step edges on Pt(210). The abundance of π-bonded ethylene appears to be a measure of corner and edge sites, similar to the abundance of ethylidyne as a measure of the number of Pt(111) oriented ensembles on a particle.[77,78]

4.5. Co-adsorption of Carbon Monoxide and Ethylene on Pt/SBA-15 Catalysts. Volumetric adsorption and DRIFTS measurements of CO and C_2H_4 demonstrated that both adsorbates influence one another. Adsorbed CO is an effective site-blocker of the adsorption of ethylene, but a Pt surface covered by an ethylidyne adlayer can be penetrated by CO. The CO/C_2H_4 layer produces a red-shift of ν(CO) relative to the CO-only surface. This suggests a significant interaction between CO and C_2H_3 directly, or one mediated through the metal surface.

Numerous studies of the co-adsorption of CO and organics conducted on single-crystal surfaces appear in the surface science literature.[82−86] These studies are often constrained to low temperatures and UHV conditions. Under these conditions, H atoms formed on the surface quickly recombine and desorb as H_2. Carbon monoxide and hydrogen co-adsorption has been studied extensively,[87−90] but it is not considered here due to the low H coverage under the experimental conditions of this study. Co-adsorption of CO and ethylene on single-crystal surfaces has shown that CO stabilizes ethylidyne[83,91] or even induces its formation on Rh surfaces lacking 3-fold symmetry.[92] The onset of ethylidyne decomposition is 50 K higher on a CO-covered Ir(111) surface versus a clean surface, which the authors suggest is related to the strong interaction between the CO and C_2H_3 dipoles.[93] Similar behavior was observed on Ru(001).[83] C_xH_y fragments from ethylidyne decomposition appeared to be more stable in the presence of adsorbed CO, perhaps suggesting that CO inhibits C−C bond cleavage.[91] These observations revealed that CO may play a complex role in catalysis beyond site blocking, such as influencing the binding strength of other surface species (reactants and intermediates). Co-adsorption studies of ethylene and CO (or NO) on Rh(111) demonstrated that the diatomic molecules adsorb on their favored sites, forcing ethylidyne to adsorb on less favored sites. The desorption of CO from an ethylidyne-covered surface remained unchanged relative to CO adsorbed on the same clean surface.[82] To explain the increased stability of ethylidyne (even though it is displaced from favored adsorption sites), we consult the proposed mechanism for ethylidyne decomposition.[80] Up to six atoms are required for ethylidyne decomposition, and the statistical probability of six vacant atoms near an adsorbed ethylidyne molecule on a CO-covered surface is low.

An interesting result of the sequential co-adsorption studies is the order-dependent nature during the formation of the adlayer (Table 2). The interaction between co-adsorbates can be discussed in terms of three potential competing effects:[92] (i) static dipole interactions (the Stark effect), (ii) charge-transfer processes mediated through the surface, or (iii) a direct chemical interaction (reaction). In the case of dipole−dipole coupling through the Stark effect, interaction between co-adsorbed CO and C_2H_4 can be excluded, since no vibrational modes of the two adsorbates are close in frequency.[94] Conversely, Somorjai and

(76) Backman, A. L.; Masel, R. I. *J. Phys. Chem.* **1990**, *94*, 5300.
(77) Paul, D. K.; Beebe, T. P.; Uram, K. J.; Yates, J. T. *J. Am. Chem. Soc.* **1992**, *114*, 1949.
(78) Beebe, T. P.; Yates, J. T. *Surf. Sci.* **1986**, *173*, L606.
(79) Wang, P. K.; Slicther, C. P.; Sinfelt, J. H. *J. Phys. Chem.* **1985**, *89*, 3606.
(80) Carter, E. A.; Koel, B. E. *Surf. Sci.* **1990**, *226*, 339.
(81) Shen, J. Y.; Hill, J. M.; Watwe, R. M.; Spiewak, B. E.; Dumesic, J. A. *J. Phys. Chem. B* **1999**, *103*, 3923.
(82) Blackman, G. S.; Kao, C. T.; Bent, B. E.; Mate, C. M.; van Hove, M. A.; Somorjai, G. A. *Surf. Sci.* **1988**, *207*, 66.
(83) Henderson, M. A.; Mitchell, G. E.; White, J. M. *Surf. Sci.* **1988**, *203*, 378.
(84) van Hove, M. A.; Lin, R. F.; Ogletree, D. F.; Blackman, G. S.; Mate, C. M.; Somorjai, G. A. *J. Vac. Sci. Technol. A* **1987**, *5*, 692.
(85) Slavin, A. J.; Bent, B. E.; Kao, C. T.; Somorjai, G. A. *Surf. Sci.* **1988**, *202*, 388.
(86) Ainsworth, M. K.; McCoustra, M. R. S.; Chesters, M. A.; Sheppard, N.; Cruz, C. D. L. *Surf. Sci.* **1999**, *437*, 9.
(87) Gland, J. L.; Fischer, D. A.; Parker, D. H.; Shen, S. *Langmuir* **1991**, *7*, 2574.
(88) Parker, D. H.; Fischer, D. A.; Colbert, J.; Koel, B. E.; Gland, J. L. *Surf. Sci.* **1990**, *236*, L372.
(89) Parker, D. H.; Fischer, D. A.; Colbert, J.; Koel, B. E.; Gland, J. L. *Surf. Sci.* **1991**, *258*, 75.
(90) Wang, H.; Tobin, R. G.; Lambert, D. K.; Fisher, G. B.; DiMaggio, C. L. *Surf. Sci.* **1995**, *330*, 173.
(91) Akhter, S.; White, J. M. *Surf. Sci.* **1987**, *180*, 19.
(92) Mate, C. M.; Kao, C. T.; Somorjai, G. A. *Surf. Sci.* **1988**, *206*, 145.
(93) Chakarov, D. V.; Marinova, T. *Surf. Sci.* **1990**, *227*, 297.
(94) Frank, M.; Bäumer, M.; Kühnemuth, R.; Freund, H. J. *J. Vac. Sci. Technol. A* **2001**, *19*, 1497.

co-workers suggested that the magnitude of $\Delta\nu$(CO) on CO−C_2H_3/Rh(111) versus CO/Rh(111) indicates a Stark effect.[92]

A study by Tang et al.[95] using high-pressure STM demonstrated that the adsorbate structures formed by co-adsorption of mTorr pressures of CO and C_2H_4 at room temperature on Pt(111) is complex. At equilibrium, a static, densely packed mixed adsorbate overlayer of CO and ethylidyne form. Steric crowding by the bulky ethylidyne contributes to the lack of adsorbate mobility on the surface. In the case of CO or ethylene only adsorption (mTorr pressures and room-temperature conditions), no adsorbate structure is identified and these adsorbates diffuse across the surface. Regions of densely packed pure CO ($(\sqrt{19} \times \sqrt{19})R23.4° - 13CO$) unit cell structures[21] formed, and upon the addition of C_2H_4 the same overlayer structure with C_2H_3 partially replacing CO was observed. Sum frequency generation (SFG) surface vibrational spectroscopy studies of CO adsorption on an ethylidyne-covered Pt(111) surface suggest that two different linear-bound CO species exist, supporting the presence of pure and mixed adsorbate adlayers.[96]

The adsorption of CO onto a C_2H_4-covered surface was reduced by ∼50% versus a clean Pt surface. Chemisorbed CO (on ethylene-covered Pt) was identified at 2050 cm^{-1}, compared to 2079 cm^{-1} on a clean surface. If CO is adsorbed initially, the chemisorption capacity of C_2H_4 is reduced by almost 100% (adsorption is totally reversible; Table 2) and results in a small perturbation of ν(CO) (not shown). In the case of CO adsorption followed by C_2H_4, it is evident that ethylene inclusion on the surface is essentially prohibited, and few adsorbates attach to the surface. Due to steric considerations, the high coverage CO unit cell may prohibit ethylene adsorption, since the van der Waals radius of ethylidyne (∼2 Å[97]) is greater than that of CO. The ability of CO to adsorb on an ethylene-covered surface is a consequence of both steric effects and adsorption affinity.

5. Conclusions

The adsorption of carbon monoxide and ethylene as well as their sequential adsorption was studied over a series of Pt/SBA-15 catalysts with monodisperse particle sizes ranging from 1.7 to 7.1 nm. The volumetric adsorption of the two molecules demonstrated that both species exist on the surface regardless of the order of adsorption but in substantially reduced amounts relative to adsorption on a clean surface. Ethylene was more sensitive to the presence of adsorbed carbon monoxide due to the dense unit cell that CO forms at high coverage, while the adsorption of ethylene on a clean metal surface leads to ethylidyne formation with an open, mobile unit cell capable of accommodating CO molecules. Infrared investigations demonstrate that π-bonded, di-σ-bonded ethylene and small amounts of ethylidyne form on small Pt crystallites (≤2 nm), with the ratio of ethylidyne to π-bonded ethylene being close to unity. On larger particles, ethylidyne was the dominant surface species, suggesting that extended (111) surface planes are required for ethylidyne formation and stabilization. Adsorption of ethylene on a CO-covered surface revealed nearly total blocking of ethylene uptake. The only observable surface species were linear-bound CO, whose position was red-shifted relative to CO adsorbed on a clean Pt surface, and ethylidyne, whose position was slightly blue-shifted relative to Pt-C_2H_3. Conversely, large changes in ν(CO) were observed when CO was adsorbed on an ethylene-covered surface. At 298 K, the CO adsorption capacity decreased by half the amount adsorbed on a clean surface and ν(CO) red-shifted considerably, suggesting a donation of electron density from adsorbed ethylidyne to carbon monoxide mediated through the metal substrate.

Acknowledgment. This work was supported by the Director, Office of Science, Office of Advanced Scientific Computing Research, Office of Basic Energy Sciences, Materials Sciences and Engineering Division, of the U.S. Department of Energy under Contract No. DE-AC02-05CH11231. The authors would like to acknowledge Professor M. A. Vannice of the Pennsylvania State University for donation of the Pt/SiO_2 catalyst and Dr. Samrat Mukherjee for its preparation. We would also like to acknowledge Exxon Research and Developmental Laboratory for donation of the Pt/Al_2O_3 sample and Professor Zoltan Paàl for the EUROPT-1 sample. R.M.R. would like to acknowledge the Ford Motor Company for financial support through a graduate fellowship administered by the Berkeley Catalysis Center.

LA702685A

(95) Tang, D. C.; Hwang, K. S.; Salmeron, M.; Somorjai, G. A. *J. Phys. Chem. B* **2004**, *108*, 13300.

(96) Chen, P.; Kung, K. Y.; Shen, Y. R.; Somorjai, G. A. *Surf. Sci.* **2001**, *494*, 289.

(97) Stacchiola, D.; Kaltchev, M.; Wu, G.; Tysoe, W. T. *Surf. Sci.* **2000**, *470*, L32.